

## Localized surface-plasmon resonances in periodic nondiffracting metallic nanoparticle and nanohole arrays

J. Parsons, E. Hendry, C. P. Burrows, B. Augu  , J. R. Sambles, and W. L. Barnes  
*School of Physics, University of Exeter, Stocker Road, Exeter, EX4 4QL, United Kingdom*

(Received 29 October 2008; revised manuscript received 27 January 2009; published 26 February 2009)

We compare the optical response of periodic nondiffracting metallic nanoparticle and nanohole arrays. Experimental data from both structures show a pronounced minimum in their wavelength-dependent transmittance that, through numerical modeling, we identify as being due to the excitation of localized surface-plasmon resonances associated with the nanoparticles/nanoholes. Our main finding is that, while the optical response of the nanoparticle arrays is largely independent of interparticle separation, the response from nanohole arrays shows a marked dependence on interhole separation. We attribute this effect to coupling between localized surface-plasmon resonances mediated by the symmetric surface plasmon-polaritons associated with the metal film. Further numerical modeling supports this view.

DOI: [10.1103/PhysRevB.79.073412](https://doi.org/10.1103/PhysRevB.79.073412)

PACS number(s): 73.20.Mf, 78.67.Bf

It is well established that metallic nanoparticles support localized surface-plasmon resonances (LSPRs) in the visible.<sup>1</sup> Such resonances have been extensively studied in recent years particularly as potential applications emerge, such as surface enhanced Raman spectroscopy<sup>2,3</sup> and biosensing,<sup>4–6</sup> applications that exploit the strongly localized electromagnetic fields associated with these resonant modes. Arrays of nanoparticles have in particular received considerable attention as advances in fabrication techniques allow finer control over structural dimensions.<sup>7–11</sup> It is also known that when metal nanoparticles are brought into close proximity to each other the modes they support may interact, or couple, so as to modify both the resonance shape and frequency of the LSPRs.<sup>12,13</sup> The properties of LSPRs associated with metallic nanoparticles can also be modified by the presence of a nearby metallic surface.<sup>14,15</sup>

The extraordinary optical transmission properties of regular arrays of nanoholes in thin metal films were first reported by Ebbesen and co-workers.<sup>16</sup> Since then it has been demonstrated that under appropriate conditions single nanoholes in metallic films may support LSPRs in a manner analogous to that of nanoparticles.<sup>17–22</sup> The similarities between the LSPRs of nanoholes and nanodiscs were discussed by Haynes *et al.*<sup>10</sup> Indeed, K  ll and co-workers<sup>17</sup> recently showed that for irregular arrays of such holes the LSPRs of the nanoholes are blueshifted as the hole density is increased, an effect attributed to coupling between LSPRs of neighboring holes. However, as far as we are aware, there has not yet been a comparison of interparticle/interhole coupling in periodic nondiffracting metallic nanoparticle/nanohole arrays. Here we present such a study and show that despite their similarities, these complementary structures show marked differences in their optical response. For the range of periods considered here, we find that the spectral position of the transmittance minimum associated with the nanohole arrays varies with the array period, an effect we attribute to strong LSPR coupling mediated by surface plasmon-polaritons (SPPs) supported by the intervening flat metallic film. For the complementary nanoparticle arrays there is little shift since SPPs are not supported by this structure. Results from numerical modeling help us identify the role of the symmetric (with respect to surface charge distributions<sup>23</sup>) SPP mode

supported by the metal film in causing this difference between hole and particle arrays. Our results are consistent with the blueshift of the LSPR noted by K  ll and co-workers<sup>17</sup> on increasing the hole density of irregular nanohole arrays.

Our structures were fabricated using focused ion-beam (FIB) milling for the hole arrays and electron-beam lithography for the particle arrays (using a modified FEI Nova 600 system). For both the holes and the particles, a glass substrate ( $n=1.52$ ) was used, on which gold (Au) films of thickness  $20 \pm 2$  nm were deposited by thermal evaporation (at a rate of  $5 \text{ \AA s}^{-1}$  and at a pressure  $1 \times 10^{-6}$  mbar). FIB milling was used to produce square arrays of circular holes with periodicities of 200, 225, and 250 nm; the arrays were  $8 \mu\text{m}$  on a side. Arrays of circular nanoparticles were fabricated using electron-beam lithography. Glass substrates were spin coated with a resist [3% polymethylmethacrylate in anisole] and soft baked for 10 min at 475 K. This was followed by exposure using a focused electron beam. After developing the sample in a mixture of propan-2-ol and water (ratio 1:3); a 20 nm Au film was then deposited by thermal evaporation. Unexposed resist was then removed using a lift-off technique, resulting in  $8 \mu\text{m}$  square arrays of Au particles. The insets in Fig. 1 show scanning electron microscope images of both 90 nm diameter hole and particle arrays, each with a periodicity of 200 nm. For this choice of period diffraction is not possible for frequencies in the vicinity of the LSPRs. Bright-field transmittance spectra were obtained by illuminating the sample with a collimated beam of light from a tungsten filament source at normal incidence. An objective (100 $\times$ ) was used to collect the light and pass it to a spectrometer. The optical responses of the arrays were simulated using a commercial finite-element package (HFSS) with a mesh size of 4.5 nm. Permittivity values for gold were taken from reference data.<sup>24</sup>

Figure 1 shows a comparison between experimental and simulated transmittance spectra for square arrays with period 200 nm of 90 nm diameter cylindrical holes [Fig. 1(a)] and 90 nm diameter cylindrical particles [Fig. 1(b)]. Also shown in Fig. 1 are simulated absorbance spectra for these two structures, together with the measured transmittance of 20 nm thick planar gold film (on glass) for comparison. We

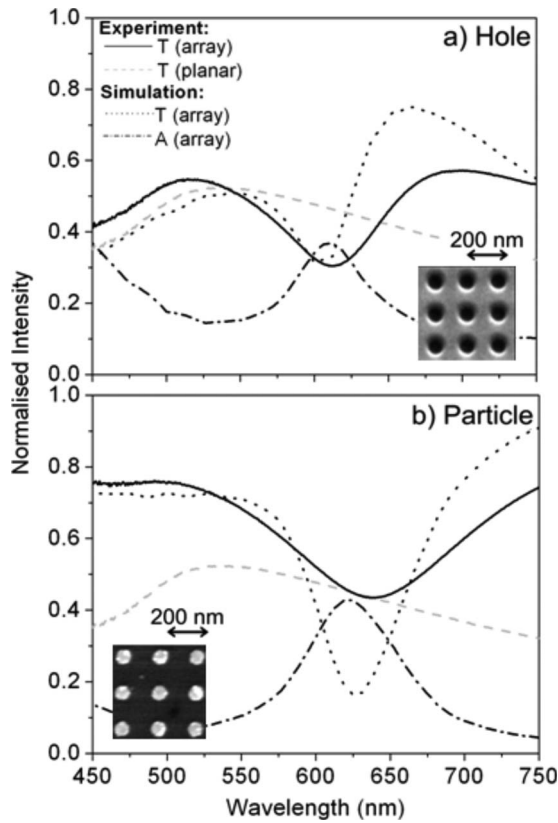


FIG. 1. Experimental transmittance spectra are compared against simulated transmittance and absorbance spectra obtained for  $8 \mu\text{m}$  square arrays of  $90 \text{ nm}$  diameter holes in a (a)  $20 \text{ nm}$  thick Au film and (b)  $90 \text{ nm}$  diameter,  $20 \text{ nm}$  height cylindrical Au particles with periodicity  $200 \text{ nm}$ , illuminated at normal incidence in air. The dashed gray curve in both (a) and (b) shows the experimental transmittance spectrum obtained from a  $20 \text{ nm}$  Au film illuminated at normal incidence in air.

chose a film thickness such that holes and particles of similar radii would have LSPR modes in the same spectral region. For both nanoparticle and nanohole arrays, transmittance minima are observed at  $\sim 600 \text{ nm}$ . We attribute these minima to the excitation of LSPRs associated with the particles and holes. Confirmation of this interpretation comes from looking at the (simulated) absorbance spectra: the absorbance spectra show clear maxima that are linked to the transmittance minima, something that is expected when resonant modes are excited, as the enhanced fields associated with the modes leads to greater absorption in the metal.<sup>25</sup> As expected, the minima in the transmittance spectra exhibit a shape typical of a Fano resonance, more easily seen when one compares the transmittance spectra with those of the planar film. For both nanoparticle and nanohole arrays there are two channels for transmission, direct transmission (a continuum), and transmission based on coupling by scattering both into and out of the LSPRs; it is interference between these two transmission routes that leads to the Fano response.<sup>26</sup> Additional numerical simulations (not shown) indicate that the resonant frequency of both hole and particle LSPR modes are angle independent, offering clear evidence that the mode is not diffractively coupled and is localized in nature.

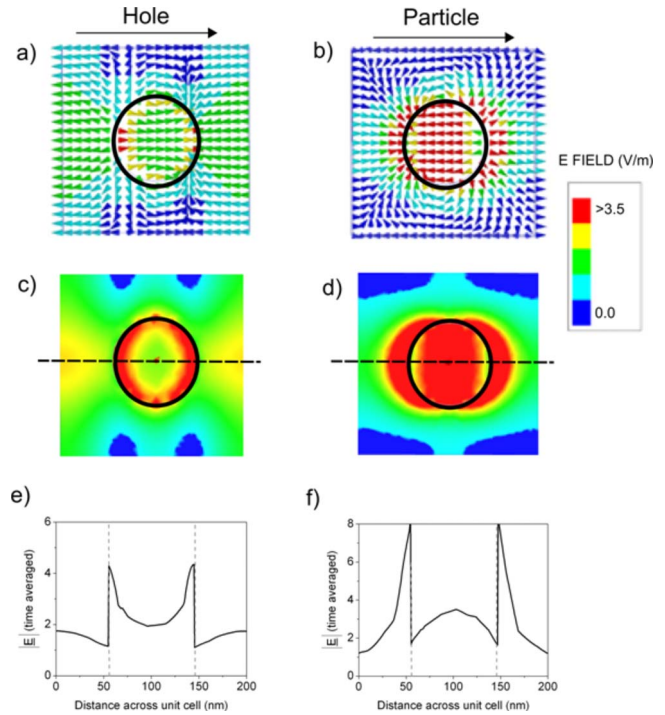


FIG. 2. (Color online). Field profiles are shown at the absorbance maximum of the hole and particle array structures. The upper profiles show the instantaneous scattered electric field vector for (a) the hole and (b) particle, taken at the same instant in phase for each structure. The arrows above (a) and (b) indicate the vector of the incident electric field. The middle plots show the time-averaged scattered electric field profiles for (c) the hole and (d) particle. In (e) and (f), a line plot has been taken through the center of the structure along the dashed lines shown in (c) and (d), and the time-averaged electric field magnitude is shown as a function of position across the unit cell.

To understand the optical response of our nanoparticle and nanohole arrays better, we carried out a number of numerical simulations of the scattered electric field in each of the structures. Similarities between the hole and particle resonant modes can be seen in Fig. 2, where we have plotted the scattered electric field distributions at the appropriate resonant frequencies. From Figs. 2(a) and 2(b) we can see that both structures exhibit a largely dipolar electric field distribution. Notice how the instantaneous electric field vectors throughout the hole array unit cell have the opposite phase when compared to those of the particle array, reflecting the complementary nature of these structures.

Interestingly, for the nanohole array, it can be seen in Figs. 2(c) and 2(e) that there is significant field enhancement at the metal-air interface in the regions *between* the holes, which is absent for the particle array [Figs. 2(a) and 2(f)]. This observation is consistent with the demonstration of the excitation of surface plasmon-polaritons of the metal film in the vicinity of nanoholes.<sup>18</sup> Of particular importance in the present case will be the nearly symmetric (with respect to surface charge distributions) SPP mode. This is the only bound SPP mode that such a thin metal film may support when flanked by different refractive index media (as is the situation here).<sup>23</sup> The field enhancement between the holes in

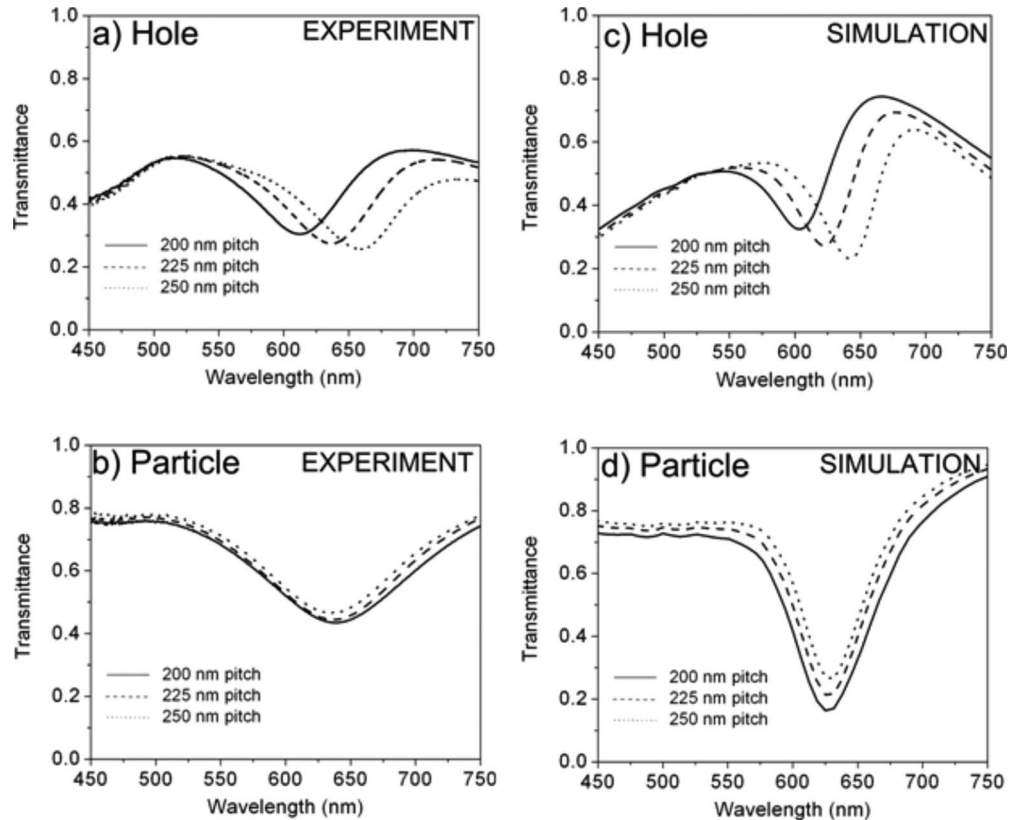


FIG. 3. Comparison between experimental and simulated transmission spectra for [(a) and (c)] 90 nm diameter hole and [(b) and (d)] particle arrays with periodicity 200, 225, and 250 nm.

Figs. 2(c) and 2(e) suggests that even in our nondiffracting arrays, nearly symmetric SPPs supported by the metal film may play an important role in determining the response. For instance, the presence of the metallic film connecting adjacent holes could provide an additional coupling mechanism between the localized resonances of nanoholes, one mediated by nearly symmetric SPPs. It is the excitation of SPPs through scattering that enables the LSPR modes of adjacent nanoholes to interact sufficiently such that a spectral shift in their response occurs.

It is well known that when metallic nanoparticles are formed into an array the LSPRs that they support may be modified due to electromagnetic coupling between the particles.<sup>10,12,13,27</sup> This coupling has been previously studied for particle arrays. Haynes *et al.*<sup>10</sup> found a small but observable blueshift in resonant frequency occurring for Au nanoparticle arrays when the period is decreased from 500 to 250 nm (for resonances at  $\sim 750$  nm): these same authors suggested that this blueshift would cease for periods somewhat below 250 nm. Figure 3 shows the experimental and simulated transmittance spectra for 90 nm diameter hole arrays and for 90 nm diameter particle arrays for three different periods 200, 225, and 250 nm. For the particle arrays, the change in resonant wavelength is very small over this range of periods (in agreement with Haynes *et al.*<sup>10</sup>), and this is also seen in the simulated data. In contrast, the resonant transmission for the hole array is much more sensitive to the period of the structure: an increase in the period of the hole

structure by 50 nm leads to a redshift of the transmittance minimum by approximately 60 nm. This result is consistent with the blueshift of the LSPR noted by Käll and co-workers<sup>17</sup> on increasing the hole density of irregular nanohole arrays.

In addition to modifying LSPR frequencies, it should be noted that the excitation of symmetric SPPs supported by the metal film in nanohole ensembles will give rise to several other effects. First, the sensitivity of the optical response of the LSPRs to interhole separation will contribute to inhomogeneous broadening. It is thus not surprising that a random ensemble of holes<sup>17</sup> exhibits a considerably broader spectral response than the periodic arrays studied here. Moreover, the delocalization of electric field in SPP modes means that, in general, one may expect to observe weaker local-field enhancements for the LSPR of nanoholes compared to the complimentary nanoparticle structures. Indeed, we observe a factor of two difference in the calculated maximum field enhancements for our nanohole and nanoparticle arrays [Figs. 2(e) and 2(f)]. We suggest that the LSPR of nanoparticles should, in general, be more suitable for applications which rely on large local enhancements of electric field, such as surface enhanced Raman scattering.

In conclusion, we have compared the optical response of nondiffracting metallic nanoparticle and nanohole arrays. We find that these two structures, though to some extent complementary, show some marked differences. In particular we have shown that in the case of nanohole arrays the spec-

tral response depends on interhole separation while there seems to be little effect of the interparticle spacing in the response of the nanoparticle array. We have suggested that this difference in response arises from an additional coupling mechanism mediated by the symmetric SPP mode that the thin metal film supports.

The authors would like to thank I. Hooper and A. P. Hibbins for many useful discussions. This work was supported through funding from Hewlett Packard (Bristol) in association with Great Western Research. W.L.B. has pleasure in acknowledging the support of the Royal Society through a Wolfson Merit Award.

- 
- <sup>1</sup>U. Kreibig and M. Vollmer, *Optical Properties of Metal Clusters* (Springer, Berlin, 1995).
  - <sup>2</sup>K. T. Carron, W. Fluhr, M. Meier, A. Wokaun, and H. W. Lehmann, *J. Opt. Soc. Am. B* **3**, 430 (1986).
  - <sup>3</sup>N. Félidj, J. Aubard, G. Lévi, J. R. Krenn, M. Salerno, G. Schider, B. Lamprecht, A. Leitner, and F. R. Aussenegg, *Phys. Rev. B* **65**, 075419 (2002).
  - <sup>4</sup>G. Raschke, S. Kowarik, T. Franzl, C. Sönnichsen, T. A. Klar, J. Feldmann, A. Nichtl, and K. Kürzinger, *Nano Lett.* **3**, 935 (2003).
  - <sup>5</sup>A. J. Haes and R. P. Van Duyne, *J. Am. Chem. Soc.* **124**, 10596 (2002).
  - <sup>6</sup>T. Rindzevicius, Y. Alaverdyan, A. Dahlin, F. Höök, D. S. Sutherland, and M. Käll, *Nano Lett.* **5**, 2335 (2005).
  - <sup>7</sup>A. Hohenau, J. R. Krenn, J. Beermann, S. I. Bozhevolnyi, S. G. Rodrigo, L. Martin-Moreno, and F. Garcia-Vidal, *Phys. Rev. B* **73**, 155404 (2006).
  - <sup>8</sup>F. J. García de Abajo, *Rev. Mod. Phys.* **79**, 1267 (2007).
  - <sup>9</sup>S. Enoch, R. Quidant, and G. Badenes, *Opt. Express* **12**, 3422 (2004).
  - <sup>10</sup>C. L. Haynes, A. D. McFarland, L. Zhao, R. P. Van Duyne, G. C. Schatz, L. Gunnarsson, J. Prikulis, B. Kasemo, and M. Käll, *J. Phys. Chem. B* **107**, 7337 (2003).
  - <sup>11</sup>S. Kim, J. Jin, Y. Kim, I. Park, Y. Kim, and S. Kim, *Nature (London)* **453**, 757 (2008).
  - <sup>12</sup>V. G. Kravets, F. Schedin, and A. N. Grigorenko, *Phys. Rev. Lett.* **101**, 087403 (2008).
  - <sup>13</sup>B. Auguie and W. L. Barnes, *Phys. Rev. Lett.* **101**, 143902 (2008).
  - <sup>14</sup>J. Cesario, R. Quidant, G. Badenes, and S. Enoch, *Opt. Lett.* **30**, 3404 (2005).
  - <sup>15</sup>W. R. Holland and D. G. Hall, *Phys. Rev. Lett.* **52**, 1041 (1984).
  - <sup>16</sup>T. W. Ebbesen, H. J. Lezec, H. F. Ghaemi, T. Thio, and P. A. Wolff, *Nature (London)* **391**, 667 (1998).
  - <sup>17</sup>J. Prikulis, P. Hanarp, L. Olofsson, D. Sutherland, and M. Käll, *Nano Lett.* **4**, 1003 (2004).
  - <sup>18</sup>C. Sönnichsen, A. C. Duch, G. Steininger, M. Koch, G. von Plessen, and J. Feldmann, *Appl. Phys. Lett.* **76**, 140 (2000).
  - <sup>19</sup>A.-L. Baudrion, F. de Leon-Perez, O. Mahboub, A. Hohenau, H. Ditlbacher, F. J. Garcia-Vidal, J. Dintinger, T. W. Ebbesen, L. Martin-Moreno, and J. R. Krenn, *Opt. Express* **16**, 3420 (2008).
  - <sup>20</sup>C. Genet and T. W. Ebbesen, *Nature (London)* **445**, 39 (2007).
  - <sup>21</sup>T. H. Park, N. Mirin, J. B. Lassiter, C. L. Nehl, N. J. Hallas, and P. Nordlander, *ACS Nano* **2**, 25 (2008).
  - <sup>22</sup>T. Rindzevicius, Y. Alaverdyan, B. Sepulveda, T. Pakizeh, M. Käll, R. Hillenbrand, J. Aizpurua, and F. J. Garcia de Abajo, *J. Phys. Chem. C* **111**, 1207 (2007).
  - <sup>23</sup>L. Smith, M. C. Taylor, and W. L. Barnes, *J. Mod. Opt.* **55**, 2929 (2008).
  - <sup>24</sup>P. B. Johnson and R. W. Christy, *Phys. Rev. B* **6**, 4370 (1972).
  - <sup>25</sup>W. L. Barnes, W. A. Murray, J. Dintinger, E. Devaux, and T. W. Ebbesen, *Phys. Rev. Lett.* **92**, 107401 (2004).
  - <sup>26</sup>C. Genet, M. P. van Exter, and J. P. Woerdman, *Opt. Commun.* **225**, 331 (2003).
  - <sup>27</sup>B. Lamprecht, G. Schider, R. T. Lechner, H. Ditlbacher, J. R. Krenn, A. Leitner, and F. R. Aussenegg, *Phys. Rev. Lett.* **84**, 4721 (2000).